Tellus (1987), *39A*, 161-169

The capture of current meander by coastal geometry with possible application to the Kuroshio Current

By TOSHIO YAMAGATA and SHIN-ICHIRO UMATANI, *Division of Ocean Hydrodynamics, Research Institute for Applied Mechanics, Kyushu University, Kasuga 816, Japan*

(Manuscript received 4 May 1985; in final form 17 June 1986)

ABSTRACT

The problem of the bimodal behavior of the Kuroshio path, south of Japan is discussed by use of the Korteweg-de Vries equation with forcing and dissipation. We show that a localized, large meander of the ocean current is produced by coastal step-like geometry when the upstream current is faster than the long Rossby wave speed. In particular, even if the forcing due to coastal geometry is weak, our dynamical system has a chance to jump from a small meander state to a large meander state because of multiple equilibria. This transition is accomplished by capturing a large, propagating disturbance. These model results are consistent, at least qualitatively, with observations of the Kuroshio.

1. Introduction

The problem of interaction of the Kuroshio Current with coastal geometry has been the subject of very intense investigation during the past few years (Charney and Flierl, 1981; Chao and McCreary, 1982; Masuda, 1982; Chao, 1984; Yasuda et al., 1985). Unfortunately, however, our understanding of the peculiar bimodality of the Kuroshio path south of Japan is still far from complete. This is partly because of the lack of systematic long-term observations and partly because of the difficulty of the problem itself. The most controversial issue has been the relation between the Kuroshio path south of Honshu and the transport upstream of Kyushu (Fig. 1). Nitani (1972), Konaga et al. (1980), and Saiki (1982), based on hydrographic data, showed that the geostrophic transport increases across the PN-line when the large-amplitude meander is present south of Honshu. Also, Kawabe (1980), based on sea level data, suggested that the meander is associated with the large upstream surface current and transport. Recently, Yamagata et al. (1985) showed that those changes of the Kuroshio are not only consistent with the interannual variability of the North Equatorial Current but also

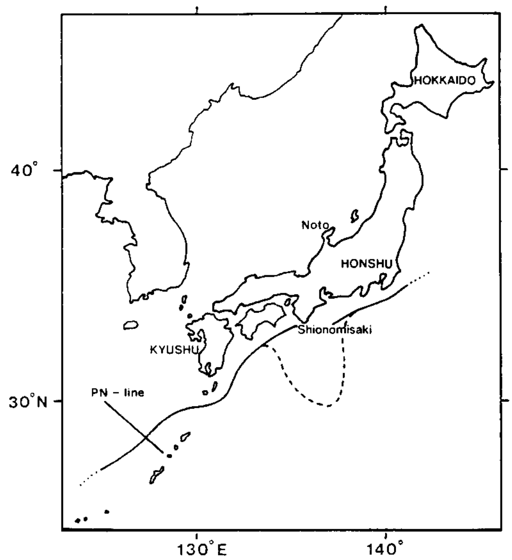

Fig. 1. Schematic patterns of the Kuroshio. The broken line shows the large meander state. The solid line shows the small meander state. The location of the hydrographic section (PN-line) is also shown.

associated with the El Niño/Southern Oscillation events. However, only Nitani (1975) claimed a positive correlation between the weakening of the Kuroshio volume transport off Cape Shionomisaki and the large-amplitude meander. As demonstrated by Taft (1972), however, the apparent decrease of the transport off Cape Shionomisaki cannot be the cause but the effect of the meander itself.

Based on the data analysis of Nitani (1975), White and McCreary (1976) suggested that the Kuroshio meander was a Rossby wave (whose phase speed is C) excited by the Kyushu coastal perturbation for *subcritical* ($U + C < 0$) or *critical* ($U + C = 0$) upstream current U. Since then, the Rossby lee-wave model appears to have been substantiated by the aforementioned modellers. One should particularly note that all these authors assume a *supercritical* ($U + C > 0$) flow as a no-meander state. As mentioned above, however, the transport off Cape Shionomisaki may not be a good index of the upstream condition; it behaves rather conversely. In addition, Nishiyama et al. (1981) showed that the warm, anticyclonic eddy east of Kyushu is weakened when the cyclonic Kuroshio meander develops south of Honshu. For this reason, the main issue we address here is: is it possible to present a localized, cyclonic meander which may exist in a *supercritical* upstream condition?

We should also notice that the special dynamical role played by Cape Shionomisaki has been overlooked in previous model studies. As reviewed by Shoji (1972), during the phase of transition from the normal state to the meander state, the initial meander off Kyushu progresses eastward at a speed of about 0.1 m s^{-1}. It is off Cape Shionomisaki that capture of the meander is observed. In addition, it is well-known that the sea level difference between Kushimoto and Uragami gives an excellent index of the interannual change of the Kuroshio path despite the proximity of the two tidal stations both located at the tip of Cape Shionomisaki (Moriyasu, 1958). According to Kawabe (1984), the sea level at Kushimoto is typical of those recorded at all tidal stations west of Kushimoto, whereas the one at Uragami is typical of those recorded at all tidal stations east of Uragami. This means that the Kuroshio flows normally very near the coast until it separates from Cape Shionomisaki. Based on these observations, we will adopt a step-like coastal geometry as a model shoreline.

The purpose of the present paper is thus to present a dynamical model of the Kuroshio meander which seems to be more consistent with the realistic changes of the upstream condition. Our model which takes the special dynamical role of coastal geometry into account turns out to be governed by the Korteweg-de Vries equation with forcing and dissipation. This model equation and its special multiple solutions are not novel; they were discussed by Patoine and Warn (1982) and Warn and Brasnett (1983) in the subject of multiple states of the atmosphere. Thus, we wish to address the issue of the Kuroshio meander with the simple model and discuss its relevance to observations.

The presentation of this paper is the following. In Section 1, we introduce simple mathematical formulation and derive the evolution equation with forcing and dissipation. Several important properties of our formalism as a theory of steady current meander are discussed by use of an analytical method (in Section 3) and a numerical method (in Section 4). Section 5 is reserved for summary of the present model results.

2. The model

For simplicity, we consider the barotropic quasi-geostrophic equation in the presence of coastal geometry on a β-plane. In the non-dimensional form it may be written

$$\left(\frac{\partial}{\partial t} + \frac{\partial \Psi}{\partial x}\frac{\partial}{\partial y} - \frac{\partial \Psi}{\partial y}\frac{\partial}{\partial x}\right)(\nabla^2 \Psi + By) = D, \quad (2.1)$$

where Ψ is the quasi-geostrophic streamfunction and D denotes the vorticity sink. The coordinates $(x, y; t)$ have been non-dimensionalized with the characteristic scales $(L, L; L/U)$, where L is the channel width and U characteristic zonal velocity. In the above, the motion is characterized by the beta parameter

$$B = \frac{\beta L^2}{U}, \quad (2.2)$$

where β denotes the meridional gradient of the Coriolis parameter. If only dissipation is the Ekman-type friction, then D may be written as

$$D = -l(\varepsilon)\gamma\nabla^2\Psi, \quad (2.3)$$

where l is a function of a small parameter ε and $l\gamma$

denotes the damping coefficient. For a detailed derivation of (2.1) and (2.3), the reader is referred to Pedlosky (1979).

Assuming that the basic zonal flow $\bar{u}$ is sustained by vorticity source against vorticity sink, one obtains the perturbation equation for $\varepsilon\psi$:

$$\left(\frac{\partial}{\partial t}+\bar{u}\frac{\partial}{\partial x}\right)\nabla^2\psi+\left(B-\frac{\partial^2\bar{u}}{\partial y^2}\right)\frac{\partial\psi}{\partial x}+\varepsilon\left(\frac{\partial\psi}{\partial x}\frac{\partial}{\partial y}-\frac{\partial\psi}{\partial y}\frac{\partial}{\partial x}\right)\nabla^2\psi=-l(\varepsilon)\gamma\nabla^2\psi. \quad (2.4)$$

The boundary conditions are

$$\frac{\partial\psi}{\partial x}=0 \quad \text{at} \quad y=0, \quad (2.5a)$$

$$\frac{\partial\psi}{\partial x}=\varepsilon\bar{u}\frac{\partial h}{\partial x} \quad \text{at} \quad y=1+\varepsilon^2 h(x), \quad (2.5b)$$

where $h(x)$ denotes the coastline geometry. Expanding $\bar{u}$ and ψ in terms of ε,

$$\bar{u}=\bar{u}_0+\varepsilon\bar{u}_1+\varepsilon^2\bar{u}_2+\cdots$$

$$\psi=\psi_0+\varepsilon\psi_1+\varepsilon^2\psi_2+\cdots, \quad (2.6)$$

and introducing strained time and space coordinates

$$T=\varepsilon^{3/2}t, \quad X=\varepsilon^{1/2}x, \quad (2.7)$$

one finds that the zeroth order problem reduces to the stationary long wave equation

$$\psi_0=A(X,T)\phi(y)$$

$$\frac{\partial^2\phi}{\partial y^2}+\left(\frac{B-\partial^2\bar{u}_0/\partial y^2}{\bar{u}_0}\right)\phi=0, \quad (2.8)$$

where A is the amplitude of the wave and is a function of X and T. Eq. (2.8) composes a well-known Strum-Liouville problem. Note that for $\bar{u}_0=$ const., (2.8) has simple modes

$$\phi=\sin m\pi y, \quad (2.9a)$$

with

$$\bar{u}_0=\frac{B}{m^2\pi^2}. \quad (2.9b)$$

Thus $\bar{u}_0$ is assumed so that an infinitely long wave (of which phase speed is $-B/(m^2\pi^2)$) is stationary. Every solution to (2.8) does not necessarily yield a valid solution. Suffice it to say that a solvability condition which arises at the next order problem constrains solutions of (2.8). The problem at the first order is then

$$\frac{\partial^3\psi_1}{\partial y^2\partial X}+\left(\frac{B-\partial^2\bar{u}_0/\partial y^2}{\bar{u}_0}\right)\frac{\partial\psi_1}{\partial X}=-\frac{\partial}{\partial T}\left(\frac{1}{\bar{u}_0}\frac{\partial^2\psi_0}{\partial y^2}\right)-\frac{\bar{u}_1}{\bar{u}_0}\frac{\partial^3\psi_0}{\partial y^2\partial X}+\frac{1}{\bar{u}_0}\frac{\partial^2\bar{u}_1}{\partial y^2}\frac{\partial\psi_0}{\partial X}-\frac{1}{\bar{u}_0}\left(\frac{\partial\psi_0}{\partial X}\frac{\partial^3\psi_0}{\partial y^3}-\frac{\partial\psi_0}{\partial y}\frac{\partial^3\psi_0}{\partial y^2\partial X}\right)-\frac{\partial^3\psi_0}{\partial X^3}-\frac{\gamma}{\bar{u}_0}\frac{\partial^2\psi_0}{\partial y^2}, \quad (2.10)$$

with boundary conditions

$$\frac{\partial\psi_1}{\partial X}=0 \quad \text{at} \quad y=0, \quad (2.11a)$$

$$\frac{\partial\psi_1}{\partial X}=\bar{u}_0\frac{\partial h}{\partial X} \quad \text{at} \quad y=1. \quad (2.11b)$$

Here the magnitude of D is assumed to be of order $\varepsilon^{3/2}$ (i.e., $l=\varepsilon^{3/2}$). The solvability condition yields

$$\frac{\partial A}{\partial T}+p\frac{\partial A}{\partial X}+qA\frac{\partial A}{\partial X}-r\frac{\partial^3 A}{\partial X^3}=f_b-\gamma A, \quad (2.12)$$

where

$$p=\frac{1}{I}\int_0^1\left\{\frac{\bar{u}_1(B-\partial^2\bar{u}_0/\partial y^2)}{\bar{u}_0^2}+\frac{1}{\bar{u}_0}\frac{\partial^2\bar{u}_1}{\partial y^2}\right\}\phi^2\,\mathrm{d}y$$

$$q=\frac{1}{I}\int_0^1\frac{\partial}{\partial y}\left(\frac{B-\partial^2\bar{u}_0/\partial y^2}{\bar{u}_0}\right)\frac{\phi^3}{\bar{u}_0}\mathrm{d}y$$

$$r=\frac{1}{I}\int_0^1\phi^2\,\mathrm{d}y$$

$$f_b=\frac{-1}{I}\left[\bar{u}_0\frac{\partial\phi}{\partial y}\right]_{y=1}\frac{\partial h}{\partial X}$$

$$I=\int_0^1\left(\frac{B-\partial^2\bar{u}_0/\partial y^2}{\bar{u}_0^2}\right)\phi^2\,\mathrm{d}y. \quad (2.13)$$

Note here that r and I are positive definite if the second derivative of the basic eastward flow $\bar{u}_0$ is small.

The above equation is an inhomogeneous form of the well-known Korteweg-de Vries equation (*cf.* Charney and Flierl, 1981). The properties of the homogeneous form of (2.12) have been applied extensively to planetary fluids since Long (1964) first introduced the intriguing idea of a shear soliton to the field of geophysical fluid dynamics (*cf.* Yamagata, 1982; Malanotte-

Rizzoli, 1982). However, it is more recently even in applied mathematics that the role of the weak inhomogeneous terms has been discussed (Karpman, 1977; Kaup and Newell, 1978). The actual process they assumed is the weak dissipation which perturbs the exactly integrable system. In (2.12), however, both forcing and dissipation are included so that one may discuss properties of multiple equilibria in a non-linear system.

Before going into details of analysis, it is convenient to introduce the transformation

$$\begin{pmatrix} A \\ X \\ T \end{pmatrix} \to \begin{pmatrix} 2r^{1/3}q^{-1}\zeta \\ r^{1/3} \quad \eta \\ T \end{pmatrix}. \tag{2.14}$$

Then (2.13) becomes

$$\frac{\partial\zeta}{\partial T} + \delta\frac{\partial\zeta}{\partial\eta} + 2\zeta\frac{\partial\zeta}{\partial\eta} - \frac{\partial^3\zeta}{\partial\eta^3} = \lambda f_b - \gamma\zeta, \tag{2.15}$$

where $\delta = p/r^{1/3}$ and $\lambda = q/(2r^{1/3})$. Since q is positive for the inshore shear of the Kuroshio, the amplitude A has the same sign as ζ.

3. Analytical results

Let us summarize solution of (2.15) under the influence of weak forcing and dissipation. By linearizing (2.15), one obtains

$$\frac{\partial\zeta}{\partial T} + \delta\frac{\partial\zeta}{\partial\eta} - \frac{\partial^3\zeta}{\partial\eta^3} = \lambda f_b - \gamma\zeta. \tag{3.1}$$

The solution is

$$\zeta = \lambda\int_{-\infty}^{\infty}\frac{\hat{f}_b(k)(-i + e^{-i\omega(k)T})}{\omega(k)}e^{ik\eta}\,dk, \tag{3.2}$$

where $\hat{f}_b$ is the Fourier transform of $f_b(\eta)$ and $\omega(k) = k^3 + \delta k - i\gamma$ is the dispersion relation. Since we retain the weak damping, the steady solution is simply reduced to

$$\zeta = -i\lambda\int_{-\infty}^{\infty}\frac{\hat{f}_b(k)\,e^{ik\eta}}{\omega(k)}\,dk. \tag{3.3}$$

Notice here that the linearized solution is proportional to the magnitude of forcing. Since we have assumed weak dissipation, three roots of $\omega(k) = 0$ reduce to

$$k_1 \sim \frac{i\gamma}{\delta},\quad k_2 \sim i\sqrt{\delta} - \frac{i\gamma}{2\delta},\quad k_3 \sim -i\sqrt{\delta} - \frac{i\gamma}{2\delta}. \tag{3.4}$$

Thus, in the case $\delta > 0$ (in other words, the eastward mean flow is slightly faster than the long wave speed), localized disturbances appear only in the vicinity of the geometry. In the case $\delta < 0$ (the eastward mean flow is slightly slower than the long wave speed), it follows that damped Rossby lee-waves are generated on the downstream side of the coastal geometry. This is because the group velocity at the resonant wavelength is approximately given by $-2\delta(>0)$. It can be shown from (3.3) that cape-like geometry is more efficient to generate Rossby lee-waves than step-like geometry. One should also notice that the root k_1 gives rise to upstream disturbances. This upstream disturbance arises as a combination of the planetary beta effect and the Ekman-type friction (Yamagata, 1976). It can be shown also from (3.3) that step-like geometry is more efficient to generate upstream disturbances than cape-like geometry.

As is well-known, the inviscid, homogeneous form of (2.15) has a free solution

$$\zeta_b = -\frac{3}{2}|A_0|\,\mathrm{cn}^2\left\{\frac{1}{2}\sqrt{\frac{|A_0|}{k^*}}\times\left[\eta - \left(\delta + \frac{1-2k^*}{k^*}|A_0|\right)T\right], k^*\right\}, \tag{3.5}$$

where cn denotes the Jacobian elliptic function, A_0 is the amplitude and k^* is the modulus which measures the relative importance of nonlinearity to dispersion (Whitham, 1974). For the limit $k^* \to 1$, one has the solitary solution

$$\zeta_b = -\frac{3}{2}|A_0|\,\mathrm{sech}^2\left\{\frac{1}{2}\sqrt{|A_0|}[\eta - (\delta - |A_0|)T]\right\}. \tag{3.6}$$

Notice here that the phase speed of this free non-linear mode is given by $\delta - |A_0|$. Since ζ_b is negative, the above mode may correspond to a cyclonic meander of the Kuroshio. One intriguing example of forced non-linear solutions of (2.15) is obtained simply by choosing the specific forcing

$$f_b \equiv \frac{\gamma}{\lambda}\zeta_b, \tag{3.7}$$

which corresponds to step-like coastal geometry when $\delta = |A_0|$ is satisfied. Then (3.5) and (3.6) are solutions of (2.15). Note that these solutions are independent of the magnitude of the forcing. The above specific examples demonstrate multiple equilibria may exist whether the forcing is isolated or periodic. It should be noted that the existence of the high amplitude state has nothing to do with the weakness of forcing and dissipation. In fact, for this solution, the left-hand side and the right-hand side of (2.15) vanish independently. This is because the non-linear free mode is being resonantly sustained by the forcing and dissipation (cf. Pierrehumbert and Malguzzi, 1984). For weak forcing and dissipation, it is not necessary for forcing to balance dissipation identically (such as (3.7)) but merely that the integral $\int_{-x}^{x} (\lambda f_b - \gamma\zeta_b)\zeta_b \, dx$ should vanish. This means that the longitudinal scale of the forced, stationary solitary wave is loosely determined by the longitudinal extent of the step-like geometry.

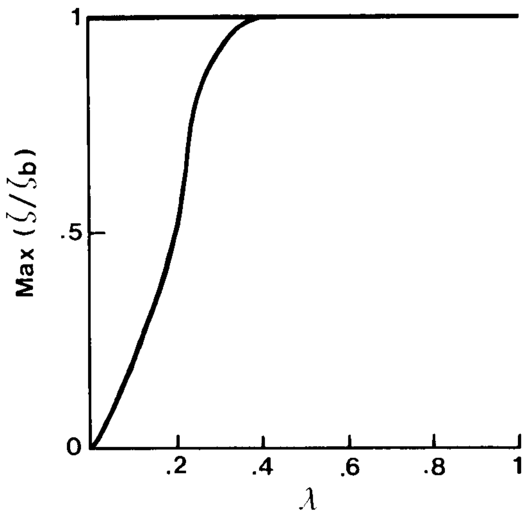

Fig. 2. The normalized magnitude of the final steady state as a function of λ.

4. Numerical simulations

4.1. Multiple equilibria

In order to apply, at least qualitatively, the results of the previous subsection to the actual oceanic phenomena, it is convenient to adopt a numerical method. We have numerically integrated (2.15) over a periodic domain of length 128 using conventional leapfrog scheme in time and centered differencing in space. We have adopted time smoothing by the restart method (every 20 steps) to control computational modes. Although there are several methods to solve the Korteweg-de Vries equation, it is known that the classical Zabusky-Kruskal scheme with a restart procedure gives fairly good results (Zabusky, 1981).

In all experiments we assumed the relation (3.7) so as to check on the effect of localized coastal geometry. In addition, except for Subsection 4.4, we assumed $\delta(=|A_0|) > 0$ in order to keep the high amplitude mode stationary. The first set of spin-up experiments is summarized in Fig. 2, where the normalized magnitude of the final steady states with the zero initial condition is plotted against λ. The damping rate was $\gamma = 0.01$. The parameter δ was fixed at the value of 1/3. It is obvious that (3.6) always satisfies (2.15). Thus it is seen that the distinct high and low amplitude equilibria can exist when the parameter λ is small. Fig. 3 shows the time evolution of the low and high amplitude equilibria obtained when starting from no initial perturbation. The final state is very sensitive to the magnitude of forcing. Namely, the high amplitude state is reached with strong forcing, whereas the low amplitude state is reached with weak forcing. Shown in Fig. 4 is the high-amplitude state obtained by initializing the model with the non-linear mode (3.6) for the same parameter set with Fig. 3. This result clearly demonstrates the existence of stable multiple states for the weak forcing.

4.2. Capture of a high state by coastal geometry

The existence of the multiple states suggests the possibility of exciting one state from another. To test this idea, we imposed a suitable high-amplitude disturbance (which satisfies the inviscid, homogeneous form of (2.15)) initially at $\eta = -5$ (upstream of the step-like geometry). Since the initial amplitude A satisfies $\delta > |A|$, the disturbance propagates eastward and stays at the forcing site after evolving into the high-amplitude stationary state (Fig. 5). If the initial amplitude of the disturbance is small enough, the high-amplitude state is never reached (not shown). Thus, it is demonstrated that the high-amplitude stationary state is excited rather rapidly by the eastward travelling disturbance with a suitable magnitude. This sudden transition reminds us of the general description of Shoji (1972) that the meander develops in a rather short time, i.e., in a few months.

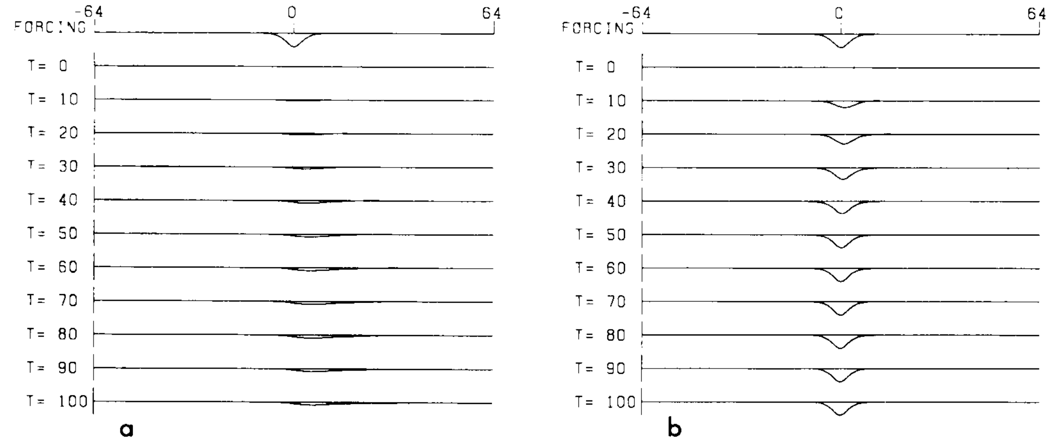

Fig. 3. Time evolution with zero initial perturbation. (a) The low amplitude case. $\lambda = 0.1$, $\gamma = 0.01$ and $\delta = 1/3$. (b) The high amplitude case. $\lambda = 0.8$, $\gamma = 0.01$ and $\delta = 1/3$.

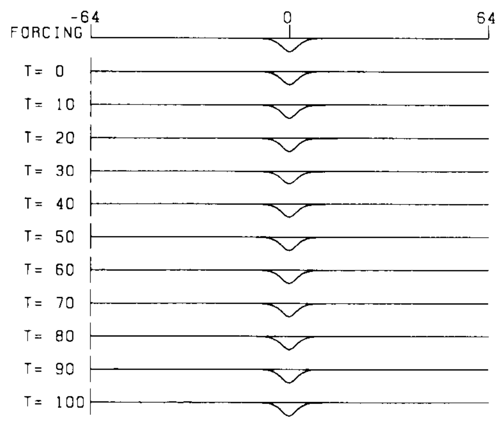

Fig. 4. Time evolution showing the stability of a high amplitude solution. This run is initialized with the high amplitude equilibrium. The parameters are set equal to Fig. 3a.

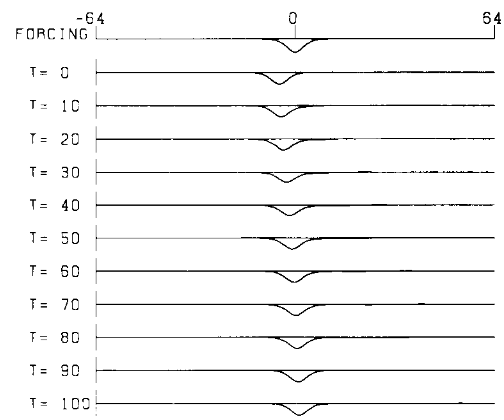

Fig. 5. Interaction of a high amplitude, damped solitary disturbance with the coastal geometry. The initial disturbance of which amplitude is 0.9 is released at $\eta = -5$. The parameters are set equal to Fig. 3a.

4.3. Inviscid response versus viscous response

So far we assumed the specific forcing given by (3.6). In the general case, forcing does not always balance dissipation even in the integral sense. One typical example is an inviscid problem. For such a case, the steady response is no longer possible. Fig. 6 demonstrates how such an inviscid system evolves. It is seen that the inviscid model emits solitons intermittently. The interval between two adjacent solitons as well as emission rate are dependent of the magnitude of forcing.

Another extreme example is provided by increasing dissipation compared to forcing. Fig. 7 shows how the high amplitude equilibrium spins down to a low amplitude equilibrium after the dissipation rate is increased at $T = 10$. Also, the high amplitude equilibrium is reduced to no meander state after the forcing is switched off (not shown). This spin-down time is given by the weak dissipation rate. In other words, the decay of the high amplitude state is a slow process. Those results remind us again of the description of Shoji (1972) that the meander decays slowly, i.e., in several years.

4.4. Subcritical ($\delta < 0$) *or critical* ($\delta = 0$) *flows*

In the case $\delta < 0$, as discussed in Section 3,

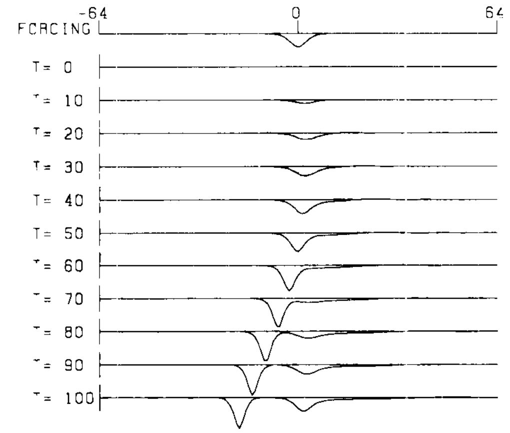

Fig. 6. Production of propagating high amplitude solitary waves by coastal geometry. $\lambda = 0.3$, $\gamma = 0$ and $\delta = 1/3$.

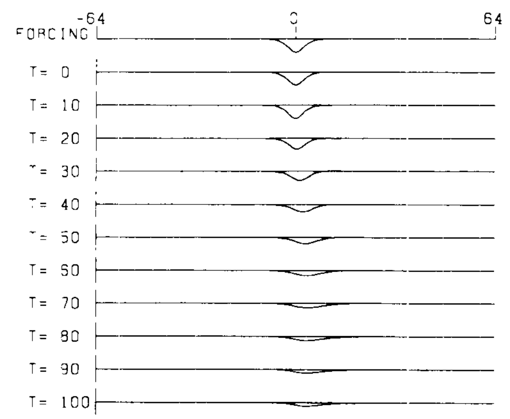

Fig. 7. Decay of a high amplitude equilibrium. The dissipation rate is increased from $\gamma = 0.02$ to $\gamma = 0.04$ at $T = 10$. $\lambda = 0.2$ and $\delta = 1/3$.

upstream disturbances and Rossby lee-waves are generated on both sides of the coastal geometry. As shown in Fig. 8, however, step-like geometry we adopted is very efficient to generate upstream disturbances (cf. Patoine and Warn, 1982). When $\gamma = 0$, they evolve into non-linear cnoidal waves (Fig. 8b). The amplitude of the cnoidal waves increases with increasing the magnitude of forcing. The wavelength, however, decreases as the amplitude increases (see (3.5)). In the case $\delta = 0$, upstream disturbances are not so remarkable compared to the case $\delta < 0$. This result is consistent with the discussion in Section 3. When $\gamma = 0$, however, a train of non-linear cnoidal waves begins to propagate westward (not shown). The behavior of this wavetrain is very similar to the case $\delta < 0$.

For our special choice of the forcing, the multiple equilibria observed in the case $\delta > 0$ were not found in the case $\delta < 0$.

5. Summary and discussion

By use of the barotropic potential vorticity equation, we have shown that a localized, large meander is produced by step-like coastal geometry in a planetary fluid flow. We have introduced several important assumptions to reduce the system to a simple model equation. Those are (i) existence of a near resonant condition ($U + C \sim 0$, where $C = -B/(m^2\pi^2)$), (ii) non-existence of a critical layer and (iii) weakness of perturbations. Since we have not examined whether those assumptions are crucial in deriving our principal results, the resulting evolution equation should be considered only as a paradigm. We hope, however, that the simplified dynamical model not only sheds some light on the more realistic, detailed experiments but also organizes various model results and field observations.

One of the most important results of our model is that the localized step-like coastal geometry can trap a solitary, large-amplitude meander provided that the basic shear flow is near resonance with a long Rossby wave. More precisely, the necessary condition that the basic flow is slightly *supercritical*, i.e., just above the phase speed of a long Rossby wave must be satisfied for the existence of multiple states. This shows quite a contrast to Charney and Flierl (1981). They adopt periodic geometry instead of localized one after deriving the forced Korteweg-de Vries equation. Thus, a zonally periodic large-amplitude meander is possible provided that the basic shear flow is slightly *subcritical*, i.e., below the value at which standing Rossby lee-waves are possible (see also Trevisan and Buzzi, 1979; Pedlosky, 1981; Wakata and Uryu, 1984). As shown in Tappert and Varma (1970) (see also Yamagata, 1983), one can derive the non-linear Schrödinger equation from the Korteweg-de Vries equation by taking a zonal wavenumber into account. This means that Charney and Flierl

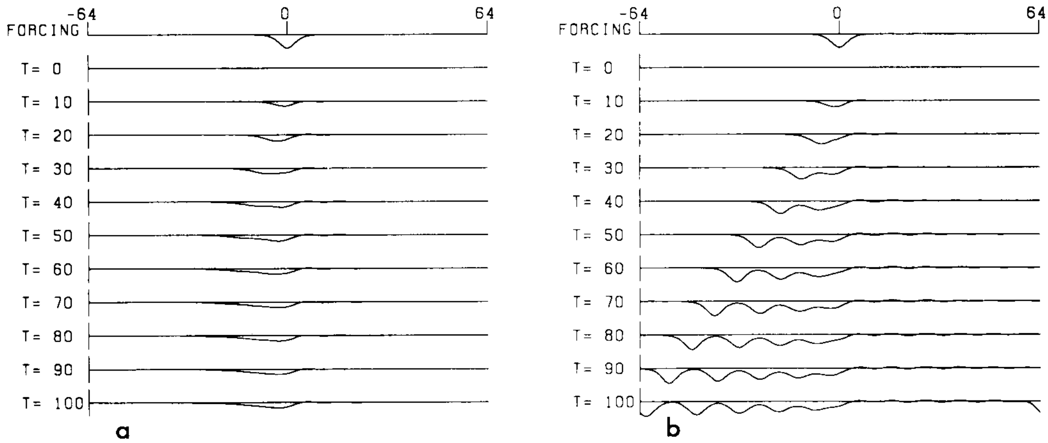

Fig. 8. Time evolution for the subcritical flow. (a) The viscous case. $\lambda = 0.5$, $\gamma = 0.05$ and $\delta = -1/3$. (b) The inviscid case. $\lambda = 0.5$, $\gamma = 0$ and $\delta = -1/3$.

(1981) discussed multiple solutions of the forced non-linear Schrödinger equation.

In our dynamical model, a non-linear large-amplitude meander can be produced locally provided that the forcing due to coastal geometry is strong under the *supercritical* condition. Even if the forcing is weak, the system still has a chance to jump from a small meander state to a large meander state because of multiple equilibria. The transition is accomplished by capturing a large propagating disturbance. This intriguing way of transition reminds us of observations reviewed by Shoji (1972). Thus one can identify the system with weak forcing as a potential meander state when the basic flow is slightly *supercritical.*

Finally, we think several assumptions we introduced need to be removed by use of a more realistic numerical model. Work along this line has already been done and will be reported soon.

6. Acknowledgements

The senior author would like to thank Professor M. Uryu who asked, "Have you completed forced problems of non-linear evolution equations?" in 1979 while preparing a paper on the long wave-short wave resonance. This question was the beginning of the whole story. He also wishes to thank Drs. R. Greatbach, R. Pierrehumbert, Y. Hayashi and S. Miyahara for useful discussions. Drs. J.-H. Yoon and M. Kawabe kindly provided opportunities of reading their preprints. The present work was partially completed while the senior author was a visiting scholar at GFDL/NOAA, Princeton University in 1984.

REFERENCES

Chao, S.-Y. 1984. Bimodality of the Kuroshio. *J. Phys. Oceanogr. 14*, 92–103.

Chao, S.-Y. and McCreary, J. P. 1982. A numerical study of the Kuroshio south of Japan. *J. Phys. Oceanogr. 12*, 680–693.

Charney, J. G. and DeVore, J. G. 1979. Multiple flow equilibria in the atmosphere and blocking. *J. Atmos. Sci. 36*, 1205–1216.

Charney, J. G. and Flierl, G. R. 1981. Oceanic analogues of large-scale atmospheric motions. *Evolution of physical oceanography*, MIT Press, 504–548.

Karpman, V. I. 1977. A perturbation theory for the Korteweg-de Vries equation. *Phys. Lett. A60*, 307–308.

Kaup, D. J. and Newell, A. C. 1978. Solitons as particles and oscillators and in slowly varying media: a singular perturbation theory. *Proc. R. Soc. London A361*, 413–446.

Kawabe, M. 1980. Sea level variations around the Nansei Islands and the large meander in the Kuroshio south of central Japan. *J. Oceanogr. Soc. Japan 36*, 227–235.

Kawabe, M. 1984. El Niño effect in the Kuroshio and western North Pacific. In *El Niño North-Niño effects in the eastern subarctic Pacific Ocean* (eds. W. S. Wooster and D. L. Fluharty). Washington Sea Grant.

Konaga, S., Nishiyama, K. and Ishizaki, H. 1980. Geostrophic transport in the eastern China Sea and southeast of Yakushima Island—a case study. *Oceanogr. Mag. 33*, 33–40.

Long, R. R. 1964. Solitary waves in the Westerlies. *J. Atmos. Sci. 21*, 197–200.

Malanotte-Rizzoli, P. 1982. Planetary waves in geophysical flows. *Advances in geophysics*, vol. 24, Academic Press, 147–224.

Masuda, A. 1982. An interpretation of the bimodal character of the stable Kuroshio path. *Deep-Sea Res. 29*, 471–484.

Moriyasu, S. 1958. On the fluctuation of the Kuroshio south of Honshu (4)—(The influence of the oceanographic conditions upon the monthly mean sea level). *J. Oceanogr. Soc. Japan 14*, 137–144.

Nishiyama, K., Konaga, S. and Ishizaki, H. 1981. Some considerations on the Kuroshio meander and the surrounding oceanographic conditions. *Pap. Meteorol. Geophys. 32*, 109–117.

Nitani, H. 1972. Beginning of the Kuroshio. In *Kuroshio, physical aspects of the Japan current* (eds. H. Stommel and K. Yoshida). University of Tokyo Press, 129–163.

Nitani, H. 1975. Variations of the Kuroshio south of Japan. *J. Oceanogr. Soc. Japn 31*, 154–173.

Patoine, A. and Warn, T. 1982. The interaction of long, quasi-stationary baroclinic waves with topography. *J. Atmos. Sci. 39*, 1018–1025.

Pedlosky, J. 1979. *Geophysical fluid dynamics*. Springer-Verlag, 624 pp.

Pedlosky, J. 1981. Resonant topographic waves in barotropic and baroclinic flows. *J. Atmos. Sci. 38*, 2626–2641.

Pierrehumbert, R. T. and Malguzzi, P. 1984. Forced coherent structures and local multiple equilibria in a barotropic atmosphere. *J. Atmos. Sci. 41*, 246–257.

Saiki, M. 1982. Relation between the geostrophic flux of the Kuroshio in the eastern China Sea and its large meanders in south of Japan. *Oceanogr. Mag. 32*, 11–18.

Shoji, D. 1972. Time variation of the Kuroshio south of Japan. In *Kuroshio: physical aspects of the Japan current* (eds. H. Stommel and K. Yoshida). University of Tokyo Press, 217–234.

Taft, B. A. 1972. Characteristics of the flow of the Kuroshio south of Japan. In *Kuroshio, physical aspects of the Japan current* (eds. H. Stommel and K. Yoshida). University of Tokyo Press, 165–214.

Tappert, F. D. and Varma, C. M. 1970. Asymptotic theory of self-trapping of heat pulses in solids. *Phys. Rev. Lett. 25*, 1108–1111.

Trevisan, A. and Buzzi, A. 1980. Stationary response of barotropic, weakly non-linear Rossby waves to quasi-resonant orographic forcing. *J. Atmos. Sci. 37*, 947–957.

Wakata, Y. and Uryu, M. 1984. Quasi-resonant Rossby wave. Part I: external wave. *J. Meteorol. Soc. Japan 62*, 388–412.

Warn, T. and Brasnett, B. 1983. The amplification and capture of atmospheric solitons by topography: a theory of the onset of regional blocking. *J. Atmos. Sci. 40*, 28–38.

Whitham, G. B. 1974. *Linear and non-linear waves*. Wiley (Interscience), 636 pp.

Yamagata, T. 1976. A note on boundary layers and wakes in rotating fluids. *J. Oceanogr. Soc. Japan 32*, 155–161.

Yamagata, T. 1982. On non-linear planetary waves: a class of solutions missed by the traditional quasi-geostrophic approximation. *J. Oceanogr. Soc. Japan 38*, 236–244.

Yamagata, T. 1983. Long non-linear topographic waves in a rotating stratified ocean. *J. Oceanogr. Soc. Japan 38*, 339–345.

Yamagata, T., Shibao, S. and Umatani, S. 1985. Interannual variability of the Kuroshio Extension and its relation to the Southern Oscillation/El Niño. *J. Oceanogr. Soc. Japan 41*, 274–281.

Yasuda, I., Yoon, J.-H. and Suginohara, N. 1985. Dynamics of the Kuroshio large meander—barotropic model. *J. Oceanogr. Soc. Japan 41*, 259–273.

Zabusky, N. J. 1981. Computational synergetics and mathematical innovation. *J. Comput. Phys. 43*, 195–249.